Index of refraction of sapphire between 24 and 1060°C for wavelengths of 633 and 799 nm

J. Tapping*

Radiometric Physics Division, Center for Radiation Research, National Bureau of Standards, Gaithersburg, Maryland 20899

M. L. Reilly

Temperature and Pressure Division, Center for Basic Standards, National Bureau of Standards, Gaithersburg, Maryland 20899

Received July 16, 1985; accepted January 6, 1986

The index of refraction of the ordinary ray in sapphire for temperatures from 24 to 1060°C and for wavelengths of 633 and 799 nm was found to be expressed to 0.02% (99% confidence level) by $n_S(T)_{633\,nm} = 1.76565 + 1.258 \times 10^{-5}T + 4.06 \times 10^{-9}T^2$ and $n_S(T)_{799\,nm} = 1.75991 + 1.229 \times 10^{-5}T + 3.10 \times 10^{-9}T^2$, where T is the temperature in degrees Celsius. These expressions were calculated from measurements of the relative change with temperature in the reflectance for a plane surface normal to the c axis of single-crystal sapphire.

INTRODUCTION

This paper reports on measurements of the relative change with temperature in the reflectance of two single-crystal sapphire samples in the range 24 to 1060°C and for light of wavelengths 633 and 799 nm. Measurements were made for a plane surface normal to the c axis of the crystal so that the results apply only to the ordinary ray. By using published values of the refractive index at 24°C,[1] our measurements are interpreted as the temperature dependence of the refractive index of sapphire at the above wavelengths.

METHOD

Measurements were made by directing laser beams onto samples of synthetic sapphire and detecting the change in intensity of the reflected beam after heating the sample to a prescribed temperature. Measurements were made at 633 nm using a helium–neon laser and at 799 nm with a krypton laser. Four arrangements of apparatus were used, all of which were variations of the one shown in Fig. 1. The variations are described below. Either laser beam could be directed along the optical path by raising or lowering the mirror M1. The beam was chopped by the chopper C to give the pulses required by the measuring equipment and then passed through the beam manipulator M2. The beam manipulator was a periscope formed by two mirrors arranged so that the emerging beam could be varied in position and direction by moving the mirrors. This allowed the beam to be accurately positioned along the optical path. At the beam splitter B approximately 10% of the beam was reflected to detector D1 to form the reference signal for the normalization of the meter readings. The transmitted beam impinged on the sample S, where a similar fraction was reflected to detector D2. The tube furnace F was moved to surround the sample for the high-temperature measurements. The ceramic tubes T, through which the beams passed, mitigated the effects of air turbulence and inhomogeneity when the furnace surrounded the sample. Not shown in Fig. 1 are several apertures that were placed along the optical path to suppress light scattered from the mirrors and beam splitter.

The samples were single-crystal sapphire disks fabricated by Insaco, Inc.,[2] from a boule grown by Crystal Systems, Inc., using the heat-exchanger method.[3] The disks had the shape shown in the inset of Fig. 1. They were nominally identical, 19 mm in diameter and of 6-mm maximum thickness. The front face of each disk was normal to the c axis of the crystal; the back face was inclined at 5° to the c axis. Both faces were ground optically flat and polished to a grade 80–50 specification.[4] For the measurements a sample rested on two parallel horizontal sapphire rods R, 3.2-mm diameter and 9.5 mm apart. The sapphire rods were used because they were rigid at high temperatures, did not contaminate the sample, and held the sample in a stable position as it was heated and cooled.

The furnace was 405 mm long with a 50-mm inside diameter. A hollow Inconel cylinder of 35-mm inner diameter and 203 mm long was placed inside to smooth the temperature gradient. The sample temperature was measured with a platinum–10% rhodium versus platinum thermocouple. The thermocouple wires were supported in high-purity twin-bore alumina tubing. To ensure that the sample was not disturbed during measurements of reflectance changes, the junction J was not placed in direct contact with the sample but close to it without actually touching it, as is shown in Fig. 1. Tests of the efficacy of the temperature measurement are described below.

The beam splitter was a third disk of sapphire nominally identical to the two samples used for the measurements. This gave a reference signal of approximately equal magnitude to that from the sample. The light signals were measured with a Laser Precision Corporation energy ratio meter, Model Rj-7200, equipped with two silicon probes, Model

0740-3232/86/050610-07$02.00

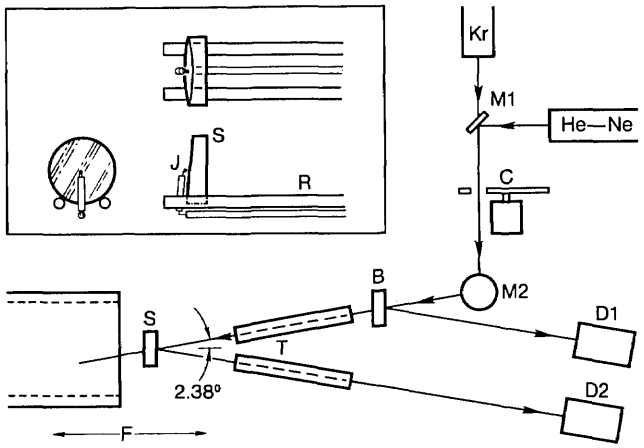

Fig. 1. A schematic layout of the apparatus used for the relative reflectance measurements. He–Ne, helium–neon laser; Kr, krypton laser; M1, mirror; C, chopper; M2, beam manipulator; B, beam splitter; T, ceramic tubes; S, sample; F, movable tube furnace; and D1 and D2, detectors. In the inset, S denotes the sample, R the sapphire support rods, and J the thermocouple junction.

RjP-765. This device was designed for measurements of laser pulses and registered only the increase in signal due to the chopped laser beam. As a consequence, readings were not susceptible to errors from background signals such as the thermal radiation from the furnace. In the mode in which it was used, the meter displayed the ratio of the magnitude of the pulse at D2 to that of the simultaneous pulse at D1 and thus represented normalized readings of the light reflected from the sample. The digital output had a resolution of one part in 1000. The meter was capable of providing a value for a single pulse or the average of 10 or 100 consecutive pulses. For these experiments the 10-pulse average was used.

The meter was interfaced with a minicomputer so that data could be logged in real time. By taking the mean of a large number of readings, it was possible to interpolate beyond the least count of the digital output.

The first series of measurements, called Setup 1 in the results given below, was made with the helium–neon laser and without the beam manipulator. Because this laser was small in size and weight, the beam could be easily positioned with the laser mounted on a small adjusting unit. For Setup 2 the large and massive krypton laser was introduced, and the beam manipulator was added. In Setup 3, a long-focal-length lens was placed between C and M2 to confine the beam, and for Setup 4 the positions of the chopper and the stops were changed.

MEASUREMENTS

First the appropriate laser beam was adjusted so that it passed down the axes of the ceramic tubes, centrally through the apertures, and impinged on the centers of the detectors. A reading was taken with the sample at ambient temperature (nominally 24°C). Then the furnace, which was preset at a particular temperature, was moved to surround and heat the sample. When the sample temperature stabilized, another reading was taken, and then the furnace was removed to allow the sample to cool. A third reading was taken when the temperature was stable at room temperature. The ratio of the hot reading to the average of the two cold readings gave one experimental value of the relative change in reflectance of the sample. One complete reading at each temperature consisted of at least 5 sets of 100 of the 10-pulse averages together with the corresponding thermocouple electromotive forces. A total of 48 readings were taken at 633 nm and 46 readings at 799 nm over the temperature range of about 400 to 1060°C.

Although the sample and its supports were the same material, they did not expand and contract at exactly the same rate because of differences in size and mass. Occasionally this resulted in slight displacement of the sample and consequently of the reflected beam. Because the silicon detectors did not have uniform sensitivity over their surfaces, beam movement could produce errors. Large movements could also cause vignetting by the ceramic tube. After each change of sample temperature, the beam position on D2 was examined, and, if there was any suspicion that it had moved, then the supports were tapped lightly to settle the sample in its proper position. If the initial and final readings at ambient temperature did not agree to about 0.1%, all three readings were discarded.

THEORY

The data collected are of the following form. If, for light of wavelength λ, $R(T_a)_\lambda$ is the reading of the meter at ambient temperature, and $R(T)_\lambda$ is the reading at temperature T, then they can be expressed as

$$R(T_a)_\lambda = k \times \rho(T_a)_\lambda \quad \text{and} \quad R(T)_\lambda = k \times \rho(T), \tag{1}$$

where $\rho(T_a)_\lambda$ and $\rho(T)_\lambda$ are the reflectances at ambient temperature and temperature T, respectively, and k is a constant. To eliminate k, we use

$$r_i(T)_\lambda = \frac{R(T)_\lambda}{R(T_a)_\lambda} = \frac{\rho(T)_\lambda}{\rho(T_a)_\lambda}, \tag{2}$$

where $r_i(T)_\lambda$ is one experimental value of the relative change in reflectance between temperature T_a and T measured at wavelength λ.

The reflectance at the air-to-sapphire interface is a function of the refractive indices of sapphire $n_S(T)_\lambda$ and of air $n_A(T)_\lambda$. To compute $n_S(T)_\lambda$ it is therefore necessary to know or assume values for $n_A(T)_\lambda$. For these calculations we used

$$n_A(T)_\lambda = 1 + 0.00028 \times 297/(273 + T), \tag{3}$$

where T is in degrees Celsius.[5,6] This is essentially the Gladstone–Dale equation,[5] and, because variations in the refractive index of air have very small effects on the experimental values of $n_S(T)_\lambda$, Eq. (3) is quite adequate for evaluating $n_A(T)_\lambda$.

The final piece of information needed to compute $n_S(T)_\lambda$ is the value of this function at one temperature. Reference 1 gives values at 24°C as functions of wavelength, and these are used in this paper.

The simplest way to compute $n_S(T)_\lambda$ is to assume that reflection took place at normal incidence so that the following formula applies[7]:

$$\rho(T)_\lambda = \left[\frac{n_S(T)_\lambda - n_A(T)_\lambda}{n_S(T)_\lambda + n_A(T)_\lambda}\right]^2. \tag{4}$$

This can be rearranged to give

$$\frac{n_S(T)_\lambda}{n_A(T)_\lambda} = \frac{1 + \rho(T)_\lambda^{1/2}}{1 - \rho(T)_\lambda^{1/2}}. \quad (5)$$

To compute an experimental value for the refractive index at T, first $n_A(T_a)_\lambda$ is found from Eq. (3), $n_S(T_a)_\lambda$ from the formula in Ref. 1, and then $\rho(T_a)_\lambda$ from Eq. (4). Next $\rho(T)_\lambda$ is found from Eq. (2), $n_A(T)_\lambda$ from Eq. (3), and, finally, $n_S(T)_\lambda$ is computed from Eq. (5).

Values of the index of refraction were also computed for reflection at the angle of incidence actually used (2.38 angular deg), employing the equations of reflection and refraction in an iterative process. The values calculated by the two methods differed by less than 0.0005%, which is significantly less than the uncertainty of the measurements.

It was also found from rigorous calculations that the orientation of the beam polarization with respect to the plane of incidence would not affect the results.

CALCULATIONS

Each experimental value, $r_i(T)_\lambda$, was first corrected for the small difference between the measured ambient temperature and the reference temperature for the calculations, 24°C.

To obtain an equation to represent the relative reflectance measurements at each wavelength as a function of temperature, polynomials of the form

$$r(T)_\lambda = 1 + \sum_{j=1}^{m} A_j(T - 24)^j, \qquad 1 \leqq m \leqq 4 \quad (6)$$

were fitted to the appropriate experimental values $r_i(T)_\lambda$ by the method of least squares. In this equation, $r(T)_\lambda$ is a function for the relative change in the reflectance of the sample at the temperature T (in degrees Celsius) to that at the reference temperature 24°C. The significance of the coefficients of each equation was tested by using an analysis of variance based on the percentile of the F distribution. We determined that the data at each wavelength were best fitted (99% confidence level) by the following quadratic equations that have been rearranged to give simple polynomials in T:

$$r(T)_{633\text{ nm}} = 0.9994 + 2.54 \times 10^{-5}T + 6.9 \times 10^{-9}T^2 \qquad (\sigma = \pm 0.00075) \quad (7)$$

and

$$r(T)_{799\text{ nm}} = 0.9994 + 2.51 \times 10^{-5}T + 5.1 \times 10^{-9}T^2 \qquad (\sigma = \pm 0.00090), \quad (8)$$

where σ is the estimated standard deviation of the residuals of each least-squares fit.

To obtain an equation for the index of refraction of sapphire at each experimental wavelength as a function of temperature, polynomials of the form

$$n_S(T)_\lambda = n_S(24)_\lambda + \sum_{j=1}^{m} B_j(T - 24)^j, \qquad 1 \leqq m \leqq 4 \quad (9)$$

were fitted by the method of least squares to the experimental values for the indices of refraction computed from the values of $r_i(T)_\lambda$ by the procedures previously described. The indices at each wavelength were best fitted by the fol-

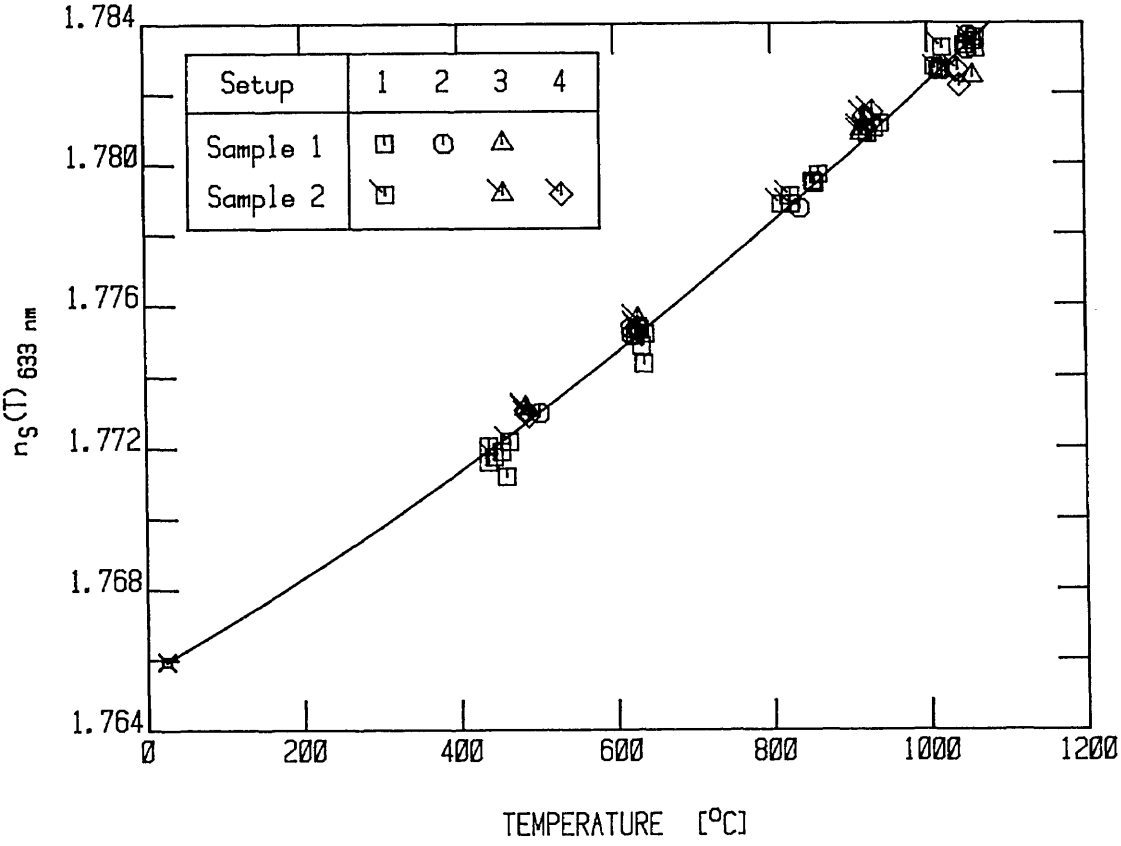

Fig. 2. The individual experimental indices of refraction for the ordinary ray in sapphire at 633 nm and the curve of the least-squares equation, $n_S(T)_{633\text{ nm}}$, versus temperature. The value of the index plotted at 24°C is taken from Ref. 1.

lowing quadratic equations, which have also been rearranged to give simple polynomials in T:

$$n_S(T)_{633\text{ nm}} = 1.76565 + 1.258 \times 10^{-5}T + 4.06 \times 10^{-9}T^2 \quad (\sigma = \pm 0.00040) \quad (10)$$

and

$$n_S(T)_{799\text{ nm}} = 1.75991 + 1.229 \times 10^{-5}T + 3.10 \times 10^{-9}T^2 \quad (\sigma = \pm 0.00047), \quad (11)$$

where σ is as defined previously.

The curve for $n_S(T)_{633\text{ nm}}$ is shown in Fig. 2 together with the individual experimental values of the refractive index from which it was derived. The corresponding quantities for 799 nm are shown in Fig. 3.

The index of refraction at each wavelength was also computed for each experimental temperature, using values for the change in relative reflectance obtained from the appropriate equation for $r(T)_{633\text{ nm}}$ or $r(T)_{799\text{ nm}}$. The difference between the index determined in this manner and that obtained from the corresponding equation for $n_S(T)_\lambda$ was ± 0.00002 or less.

The 99% confidence intervals of the equations for the refractive index were calculated by using the following procedure: Apply standard least-squares theory[8] to Eq. (9) for a temperature T

$$\mathrm{Var}(n_S) = \mathrm{Var}(B_1) \times (T - 24)^2 + \mathrm{Var}(B_2) \times (T - 24)^4 + 2\,\mathrm{Cov}(B_1, B_2) \times (T - 24)^3, \quad (12)$$

where Var and Cov signify the variance and the covariance, respectively, of the succeeding quantities in parentheses. Then at temperature T the 99% confidence interval of the corresponding value of the refractive index obtained from the least-squares equation is given by $n_S(T)_\lambda \pm C$, where

$$C = t_{k-2,0.995}\,\mathrm{Var}[n_S(T)_\lambda]^{1/2}, \quad (13)$$

k is the sample size and $t_{k-2,0.995}$ is the Student t factor for $k - 2$ degrees of freedom at the 99% confidence level. The confidence intervals of the two equations for the index of refraction are shown in Figs. 4 and 5 together with the deviations, $\Delta n_S(T)_\lambda$, of the individual experimental values from the respective equation.

SOURCES OF ERROR

Meter

A nonlinearity in the ratio meter will cause an error in the results if no correction is applied for it. In other words, the meter readings must accurately or predictably reflect the changes in the ratio of the signals at the two detectors. The nonlinearity of the Rj-7200 meter was measured with a modified form of the apparatus shown in Fig. 1. With the furnace removed and one sample at the position S, the other sample was placed behind it so that the second sample also reflected a portion of the beam on to D2. Shutters were placed so that the two beams could be intercepted independently. The meter reading for the two beams together was then compared with the sum of the readings of the individ-

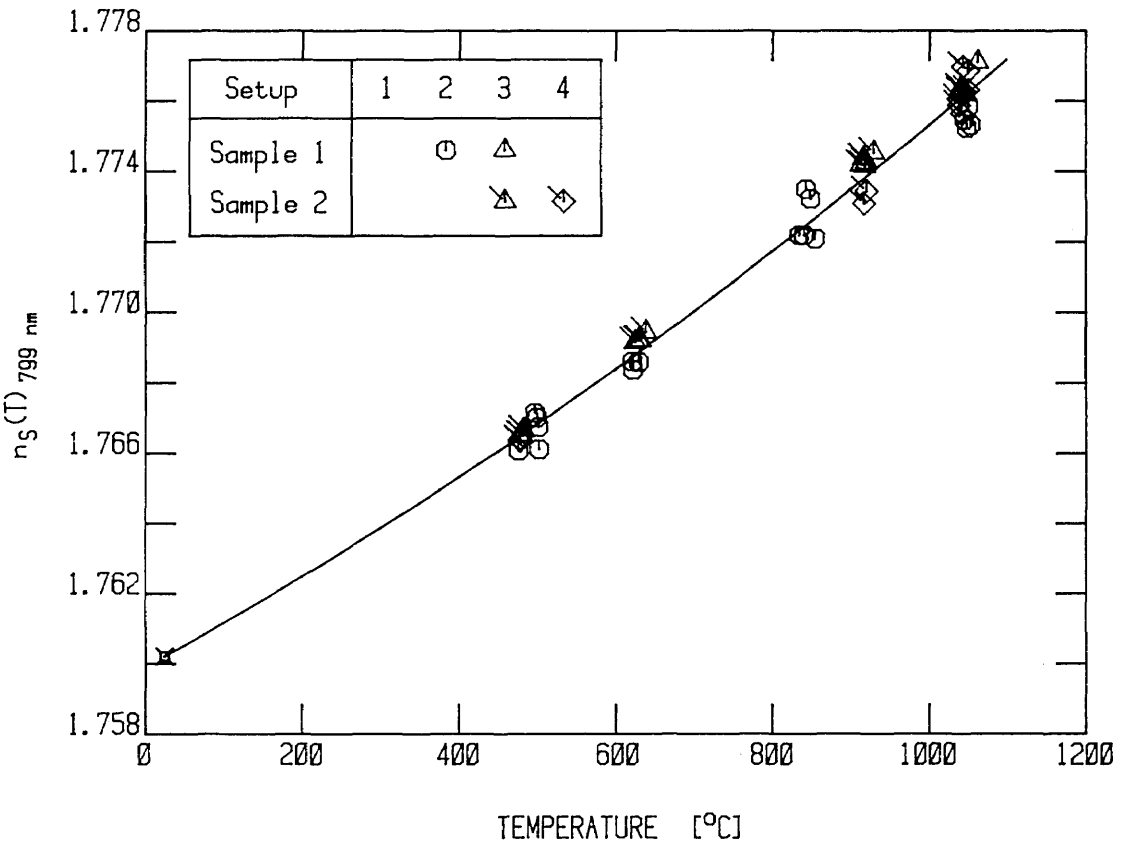

Fig. 3. The individual experimental indices of refraction for the ordinary ray in sapphire at 799 nm and the curve of the least-squares equation, $n_S(T)_{799\text{ nm}}$, versus temperature. The value of the index plotted at 24°C is taken from Ref. 1.

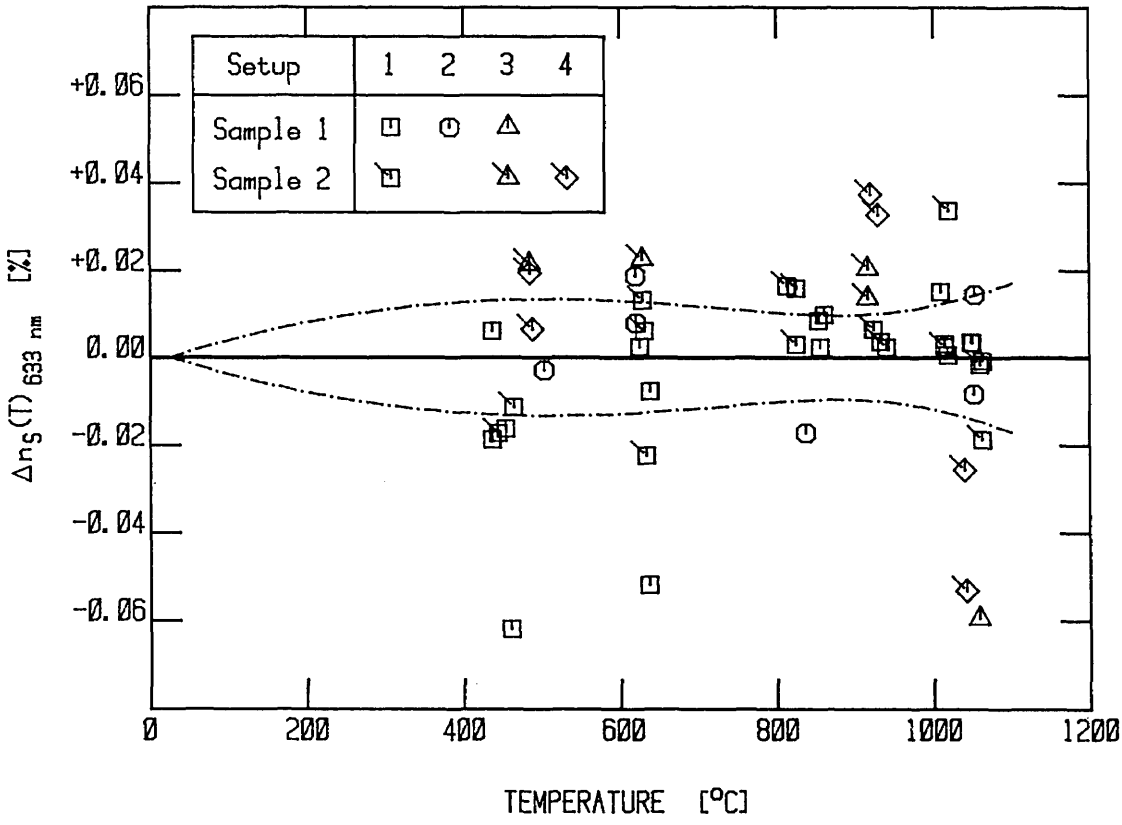

Fig. 4. $\Delta n_S(T)_{633\ nm}$, the deviations (in percent) of the individual experimental values of the refractive index of sapphire at 633 nm from the least-squares equation fitted to the data. Dashed curves, the bounds of the 99% confidence interval for Eq. (10).

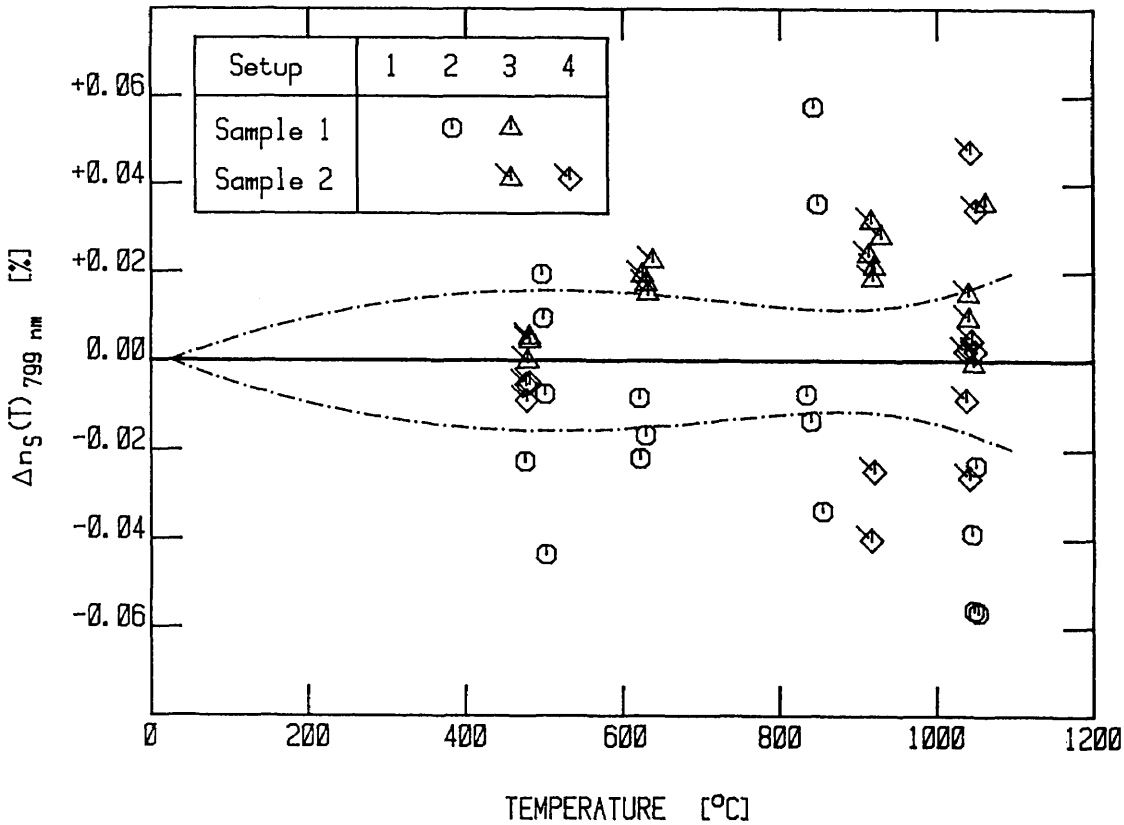

Fig. 5. $\Delta n_S(T)_{799\ nm}$, the deviations (in percent) of the individual experimental values of the refractive index of sapphire at 799 nm from the least-squares equation fitted to the data. Dashed curves, the bounds of the 99% confidence interval for Eq. (11).

ual beams to determine any nonlinearity. Our measurements indicated that, for both wavelengths, the meter was linear to better than one least count (0.1%) for a change in signal of a factor of approximately 2. Taking the nonlinearity error in the measured value to be proportional to a power function of the actual ratio,[9] a maximum nonlinearity of 0.1% for a change in signal of a factor of 2 would give an error of 0.003% for the maximum change of 1.03 recorded in the reflectance measurements.

Temperature Measurement

The thermocouple used in the measurements was calibrated by the National Bureau of Standards (NBS) Temperature and Pressure Division with an uncertainty of ±0.5°C, which was more than adequate for our purposes.

A number of tests were performed to check whether the temperature measurements were valid. The thermocouple was moved to scan along the axis of the furnace (without the sample in place) to measure the gradient in the region where the sample would be placed for the relative reflectance measurements. The gradients measured increased from the front of the furnace to the back and varied from about 2°C/cm^{-1} at 600°C to 4°C/cm^{-1} at 1100°C. During most of the reflectance measurements, the thermocouple junction was behind the sample, as is shown in Fig. 1. This placed the junction about 6 mm from the front face where the reflection occurred. The measured gradients indicate that the temperature measurements were in error by no more than 2°C.

For one set of measurements on sample 2 at 799 nm, the thermocouple junction was placed in front of the reflectance face of the sample, and no significant difference could be seen between those readings and the ones taken with the thermocouple behind the sample.

For a final test, a hole 1.3 mm in diameter and 4 mm deep was drilled into the back face of sample 1. With the sample in position, the thermocouple end was bent so that the junction was at the bottom of the hole but could be removed from the hole to the air adjacent to the sample by moving the alumina tubing along its axis. At 550°C the air temperature was found to be about 2.5°C higher than the sample temperature, whereas at 1050°C the difference was about 1.5°C.

From the above tests it was concluded that the temperature-measurement uncertainty was about 2.5°C. The slopes of the equations fitted to the experimental data are such that a 2.5°C temperature variation would change the relative reflectance by less than 0.008% and the refractive index by less than 0.004%.

Stray Light

The meter responded only to pulses of light that were synchronized with the chopped beam, so that any stray light producing an error must have originated from this beam. One possible source of this was the beam's being transmitted through the sample, impinging on the furnace walls, and then being scattered back into the optical path. This effect was tested by rotating the sample about its axis so that the beam passed through the furnace without touching the walls. A number of measurements were made with the sample in this position without any noticeable change in the results. (The sample was used in the orientation shown in Fig. 1 because its physical position was then more stable.)

A second source of stray light that was synchronized with the chopped beam and was present only during measurements with the heated sample was the furnace radiation propagated back along the optical path to the laser mirror where it was reflected as an added component of the laser beam. This added component was estimated from a worst-case calculation (i.e., with the furnace at 1060°C and no attenuation of the component) to be not larger than 5×10^{-12} J per pulse. Typical pulses detected for the helium–neon beam were approximately 2×10^{-7} J, and those for the krypton beam were approximately 1×10^{-7} J. No significant systematic error is associated with this source of stray radiation.

The effect of stray light from other sources was tested by placing apertures and shielding along the optical path and by inserting a long-focal-length lens to confine the beam. These rearrangements are the setups referred to in the figures showing the results, and it can be seen that there are no large systematic differences between them. Statistical analyses supported this observation.

Refractive Index of Air

The Gladstone–Dale formula is a good approximation to the effect of temperature on the refractive index of air. The error in the coefficient used in Eq. (3), $297/(273 + T)$, is likely to be in error by no more than 2%,[5,6] which would produce an error in the relative reflectance of the sample of less than 0.003%, which is negligible.

Refractive Index of Sapphire at 24°C

Reference 1 gives no uncertainties for the value of the refractive index of sapphire, but the results are quoted to five decimal places, and the least-squares equation presented agrees with the individual results to about one in 10^5 in the wavelength region of interest here. It seems reasonable to assume that the uncertainity is no greater than 4 parts in the fifth decimal place, or 0.002%. To a first approximation, an error in $n_S(T_a)_\lambda$ will produce the same percentage error in $n_S(T)_\lambda$, so the error component that is due to $n_S(T_a)_\lambda$ was taken as 0.002%.

Sample Surface

The surface of the sample was cleaned before the first measurement and occasionally thereafter with a lens tissue soaked in high-purity methanol. In some instances following this procedure, the reflectance of the face of the disk apparently changed during the first heating but not in subsequent ones. It was concluded that the heating removed any remaining contaminants, so that measurements were indeed made on a clean sapphire surface. This theory was supported by agreement between readings for the two samples and their long-term stability.

Random Errors

The random errors of the measurements, which include fluctuations in meter readings, changes in measured temperatures, and variations caused by changes in the arrangement of the apparatus, exhibit themselves as the scatter in the results and hence in the uncertainties of the least-squares equations fitted to the data. It can be seen in Figs. 4 and 5 that the maximum values of the confidence intervals are

about ±0.014% for $n_S(T)_{633\ nm}$ and ±0.017% for $n_S(T)_{799\ nm}$. For the equations fitted to the relative reflectance data, the maximum values of the 99% confidence intervals were ±0.046% for $r(T)_{633\ nm}$ and ±0.055% for $r(T)_{799\ nm}$.

UNCERTAINTIES

Summing in quadrature the maximum values of the 99% confidence limits shown in Figs. 4 and 5 with the estimated error for nonlinearity, temperature measurement, refractive index of air, and the refractive index of sapphire at 24°C gives ±0.016% for $n_S(T)_{633\ nm}$ and ±0.019% for $n_S(T)_{799\ nm}$. Other possible errors that have not been included are likely to be small so that they would not significantly increase the overall uncertainties, but, to ensure that the uncertainties in the refractive index are overestimates, they are claimed to be 0.02% (99% confidence level) for both wavelengths.

DISCUSSION

The only other measurement on $n_S(T)_\lambda$ at high temperatures that was found in the literature was that in Ref. 10, where it was stated that the value increases between ambient temperature and 1700°C by about 0.05 (+0.01, −0.03) in the region 0.56 to 4 μm. This agrees with the results presented here, but it is a relatively inaccurate measurement.

In Ref. 1 the average value of the temperature coefficient, $d/dT[n_S(T)_\lambda]$, for the visible-wavelength region as obtained from measurements at 17°, 24°, and 31°C is given as $1.3 \times 10^{-5}°C^{-1}$. This agrees with the values for 24°C of $1.28 \times 10^{-5}°C^{-1}$ at 633 nm and $1.25 \times 10^{-5}°C^{-1}$ at 799 nm for the equations given above.

ACKNOWLEDGMENTS

We wish to thank the following people for their contributions to this project: Jon Geist of the NBS Radiometric Physics Division for the original concept and advice during measurements, Mark Berman of the Commonwealth Scientific and Industrial Research Organization, Australia (CSIRO) Division of Mathematics and Statistics for guidance on the statistical treatment of the results, and Walter Bowers of the NBS Temperature and Pressure Division for construction of apparatus. The work was done while J. Tapping was a Guest Worker in the NBS Radiometric Physics Division, and he would like to thank the members of that division for their assistance.

*Present address, Division of Applied Physics, CSIRO, P.O. Box 218, Linfield, New South Wales 2070, Australia.

REFERENCES AND NOTES

1. I. H. Malitson, "Refraction and dispersion of synthetic sapphire," J. Opt. Soc. Am. **52**, 1377–1379 (1962).
2. Certain commercial equipment and materials are identified in this paper in order to specify the experimental procedure adequately. Such identification does not imply recommendation or endorsement by the National Bureau of Standards, nor does it imply that the equipment or materials are necessarily the best available for the purpose.
3. C. P. Khattak and F. Schmid, "Growth of large-diameter crystals by HEM for optical and laser applications," Proc. Soc. Photo-Opt. Instrum. Eng. **505**, 4–8 (1984).
4. Scratch and dig standard for specification of optical surface quality (see military specification MIL-0-13830A, 1963).
5. J. R. Partington, *An Advanced Treatise on Physical Chemistry*, Vol. 4, *Physico-Chemical Optics* (Longmans, New York, 1953), p. 8.
6. E. W. Washburn, ed., *International Critical Tables of Numerical Data, Physics, Chemistry and Technology* (McGraw-Hill, New York, 1930), Vol. VII, pp. 2–4.
7. M. Born and E. Wolf, *Principles of Optics*, 4th ed. (Pergamon, New York, 1970), p. 42.
8. M. Draper and M. Smith, *Applied Regression Analysis*, 2nd ed. (Wiley, New York, 1981).
9. H. J. Jung, "Spectral non-linearity characteristics of low noise silicon detectors and their application to accurate measurements of radiant flux ratios," Metrologia **15**, 173–181 (1979).
10. D. A. Gryvnak and D. E. Burch, "Optical and infrared properties of Al_2O_3 at elevated temperatures," J. Opt. Soc. Am. **55**, 625–629 (1965).